Available online at www.sciencedirect.com

ScienceDirect

Procedia CIRP 43 (2016) 130 – 135

www.elsevier.com/locate/procedia

14th CIRP Conference on Computer Aided Tolerancing (CAT)

3D Tolerance Analysis with manufacturing signature and operating conditions

Andrea Corrado[a], Wilma Polini[a,]*, Giovanni Moroni[b], Stefano Petrò[b]

[a]*Department of Civil and Mechanical Engineering, Università di Cassino e del Lazio Meridionale, via G. di Biasio 43, 03043 Cassino, Italy*
[b]*Dipartimento di Meccanica, Politecnico di Milano, via La Masa 1, 20156 Milano, Italy*

* Corresponding author. Tel.: +39-0776-2993679; fax: +39-0776-2993546. *E-mail address:* polini@unicas.it

Abstract

The present work shows a method to integrate the manufacturing signature and the operating conditions into a model for 3D tolerance analysis of rigid parts. The paper presents an easy way to manage the actual surfaces due to a manufacturing process and the operating conditions, such as gravity and friction, inside the variational model for a 3D tolerance analysis. The used 3D case study is deliberately simple in order to develop a conceptual demonstration.
The obtained results have been compared with those due to a geometrical model that reproduces what happens during assembly. It has been considered as reference case.

Peer-review under responsibility of the organizing committee of the 14th CIRP Conference on Computer Aided Tolerancing
Keywords: 3D tolerance analysis, manufacturing signature, friction, gravity

1. Introduction

Tolerance analysis is a critical step to design and to manufacture a product. In fact, the need to assign dimensional and geometric tolerances to assembly components is due to the standardization of production and to the correct function of the assembly. The appropriate allocation of tolerances among the different parts of an assembly can result in lower costs per assembly and higher probability of fit, reducing the number of rejected parts or the amount of rework required on components.

Practically, dimensions and tolerances of assembly components combine, according to the assembly sequences, and generate the tolerance stack-up functions. Solving a tolerance stack-up function means to determine the nominal value and the tolerance range of a product function by combining the nominal values and the tolerance ranges assigned to the assembly components.

Many approaches for tolerance analysis exist in literature for rigid assemblies [1-2], but no one of them is completely and univocally accepted. Moreover, they reduce geometric deviations to translational and rotational part feature defects, and therefore they neglect form deviation [3-5].

In contrast to that, Samper et al. take into account form deviations of planar features in the computation of assemblies [6]. The approach is based on the modal description of form defects and the simulation results depend on the approximation of form deviations by eigenmodes. This limitation is overcome in the approaches by Stoll et al. [7,8], which are based on surface registration techniques.

However, these approaches can only handle discrete geometry representation schemes, which are not able to simulate the assembly behavior of variant parts based on their point cloud representation. Since point clouds are commonly obtained by assembly and measurement applications, their consideration in CAT tools is highly desirable to enable the connection among design, manufacturing and inspection. It has been developed a skin model inspired framework for the tolerance analysis [9, 10], which is based on a representation of non-ideal workpieces employing, such as point clouds. A further work uses Legendre-Fourier polynomials to model cylindricity error into a Jacobian-Torsor model for tolerance analysis [11].

In a previous work the authors developed a geometric approach to take into account form deviation, together with

Peer-review under responsibility of the organizing committee of the 14th CIRP Conference on Computer Aided Tolerancing
doi:10.1016/j.procir.2016.02.097

those due to location and orientation, in such a way to satisfy the Geometric Product Specification standards [12].

In the following, two approaches for the relative positioning of discrete geometry skin model shape for the application in computer-aided tolerance analysis are introduced, discussed and compared. The main contributions can be found in the development of a skin model shape based on a manufacturing signature, i.e. a systematic pattern that characterizes all the features manufactured by a process, and in the creation of an approach for assembly simulation of point-cloud skin model shapes taking into account gravity and friction.

The first approach consists of a geometrical tolerance analysis that takes into account both the manufacturing signature and the operating conditions, gravity and friction, during the assembling. It should numerically reproduce what happens in the actual assembling and, therefore, it represents the reference case.

The second approach is based on the variational model, that has been introduced and developed by Martino and Gabriele [13], Boyer and Stewart [14] and Gupta and Turner [15]. The idea is to represent the variability of an assembly, due to tolerances and assembly constraints, through a parametric mathematical model. It represents the dimensional and geometrical variations affecting a part by means of differential homogeneous transformation matrices. The variational model considers dimensional and geometrical tolerances applied to some critical points (contact points among profiles belonging to coupled parts) on the surface of the assembly components. These points are generally considered uncorrelated, since the ideal surface is taken into account.

In a previous work these two approaches have been applied to a 2D case study [16]. In this paper these approaches are discussed and applied to a 3D case study in the field of computer-aided tolerance analysis.

The paper is organized as follow: in Sec. 2, the reference case study is presented. In Sec. 3, the geometrical approach with manufacturing signature and operating conditions is deeply described. In Sec. 4, the variational model with manufacturing signature and operating conditions is discussed. Finally, in Sec. 5, the results are compared and discussed.

2. 3D Case study

The considered case study is constituted by three components: a hollow box and two spheres (SPH_1 and SPH_2), as shown in Fig. 1. A dimensional and a geometrical tolerances are applied to each sphere, while the box is considered nominal. The aim is the measurement of the gap g between the upper sphere and the top side of the box as a function of the tolerances applied to each component.

Each sphere has been simulated by a set of evenly distributed points, i.e the skin model shape. The amplitude of this set is equal to 235.822, i.e. it corresponds to a value of zenit and azimut angular steps equal to 0,45°, since it seems to be sufficiently large to simulate the assembling without slowing down too much the simulation. To each point of the sphere it has been applied the following error model:

$$|\mathbf{P_i} - \mathbf{O}| = R + r + d \tag{1}$$

where $\mathbf{P_i}$ is the generic point of the circular profile, $\mathbf{O}$ is the centre of the circle, R is the nominal value of the radius of the sphere (equal to 20 mm), r is the value due to the dimensional tolerance (equal to 0,0145 mm) applied to each sphere, and d is the value due to the manufacturing signature that should keep inside the form tolerance (equal to 0,0145 mm) applied to the spheres.

The r parameter has a Gaussian density function with mean value equal to zero and standard deviation equal to a sixth of the dimensional tolerance range.

The manufacturing signature on each sphere has been represented by means of a Simultaneous Autoregressive Model of first order SAR(1). This model has been chosen because it is suitable to simulate phenomena that are spatially correlated in more than one dimension. Traditional time series models, as the ARMAX model adopted in the 2D case [13], can represent correlation only along a single direction. The SAR(1) model instead can consider the spatial structure of the lattice defined by the triangulation of the points on the surface of the sphere at their nominal coordinates to generate a spatially correlated set of deviations from perfect sphericity. The SAR(1) model has been considered, rather than other higher order models in this first application, because it is easy to build and suitable to simulate deviations on a finite number of points.

In a SAR(1) model the deviations from perfect sphericity are simulated by means of the following equation:

$$d = (\mathbf{I} - \mathbf{G})^{-1}\boldsymbol{\varepsilon} \tag{2}$$

where $\mathbf{I}$ is the identity matrix, $\mathbf{G}$ is a weight matrix and $\boldsymbol{\varepsilon} \sim N(0, \sigma^2\mathbf{I})$ is a white noise. σ is equal to 0,0024 mm.
In particular, $\mathbf{G} = \rho\mathbf{W}$. ρ is a correlation coefficient. Higher values of ρ denote a higher degree of spatial correlation among nearby points. Its value is 0,9. $\mathbf{W}$ is a neighbourhood matrix defined based on the triangulation of the points on the surface of the sphere. In particular,

$$w_{ij} = \frac{\frac{I_{ij}}{d_{ij}}}{\sum_k \frac{I_{kj}}{d_{kj}}} \tag{3}$$

in which d_{ij} is the Cartesian distance between the $\mathbf{P_i}$ and the $\mathbf{P_j}$ points of the sphere, and I_{ij} is an indicator variable, which denotes whether points i and j are neighbours, that is

$$I_{ij} = \begin{cases} 1, \text{if point } i \text{ and } j \text{ belong to a same triangle} \\ 0, \text{otherwise} \end{cases} \tag{4}$$

An example of a sphere is shown in Fig. 2.

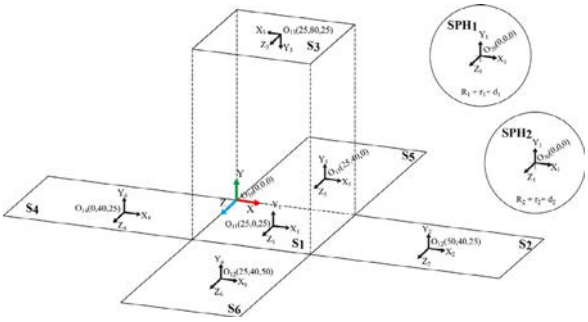

Fig.1. Datum reference frames of case study

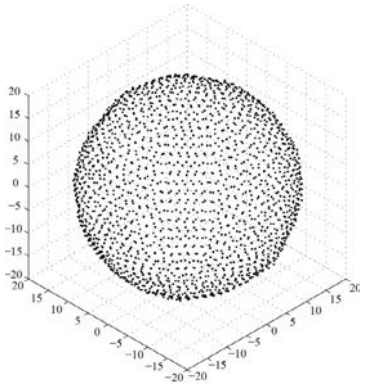

Fig. 2. SAR(1) cloud (dimension in mm, amplified 100 times)

3. Geometrical model

Two spheres have been generated by means of eq. (1) and they have been casually rotate around the X_i, Y_i and Z_i axes of a reference system that is placed in the centre of gravity of each clouds (see Fig. 3). The centre of gravity of each sphere has been calculated by the arithmetic mean of all the points' coordinates. An absolute X-Y-Z reference system is placed at the intersection among the left, the back and the bottom sides of the box, as shown in Fig. 1. The coordinates of the points constituting the first sphere are analyzed to identify the points of contact with the bottom (S_1), the left (S_4) and the back (S_5) sides of the box (A, B, C in Fig. 3). Then, the first sphere is brought into contact with the box in the identified points of contact.

Therefore, the coordinates of the points constituting the second sphere are analyzed to identify the points of contact with the sides of the box, for example with the right (S_2) and the back (S_5) sides of the box (F and E in Fig. 3).

To identify the point of contact with the first sphere, the zones on the spheres, where the probability of contact is the highest, are defined. They are a surrounding of the nominal point of contact. Then, the couples of faced points have been identified, as those points having the same x and z coordinates on the two contact zones. The minimum distance between each couple of faced points (called d_{min} in Fig. 4a) defines the couple of points that are the points of contact between the two spheres. All the points of the second sphere are shifted by the minimum distance along Y-axis to bring the second sphere into contact with the first sphere just inserted in the box, as shown in Fig. 4b.

Once assembled, it is evaluated if the general position of each sphere is stable. The condition of balance among the forces is expressed by requiring that they pass through the same point. Therefore, considering the weight force applied in the centre of gravity of the clouds (G_1 and G_2 in Fig. 4b), the reactions are applied to the points of contact and they are directed toward the centre of gravity of the sphere. The angles among these reactions and the normal vectors to the surfaces are β_1, β_2, β_3, β_4, β_5, β_6, as shown in Fig. 4b. Those six angles should have a value smaller than the static friction limit angle in order to have a stable position of the sphere; for steel components they should be smaller than 2°.

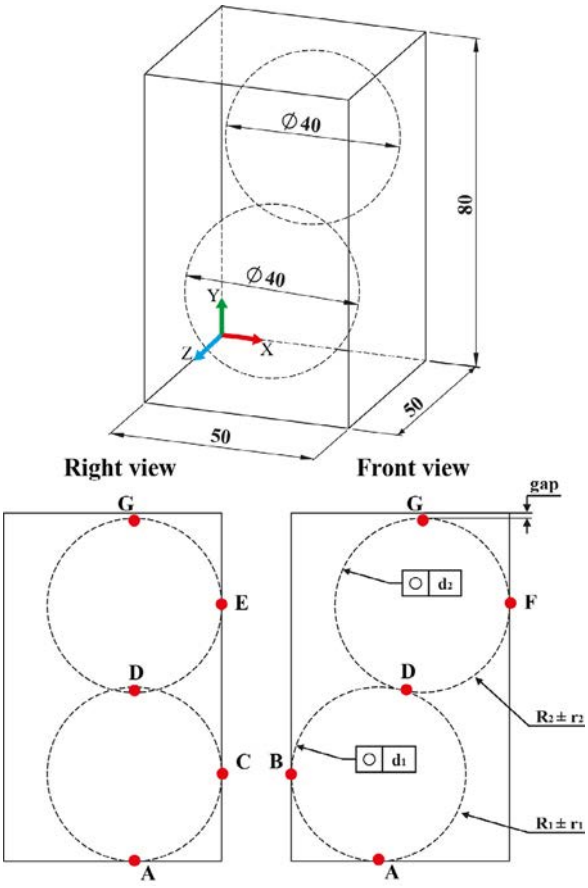

Fig. 3. 3D case study

Otherwise, the sphere rotates until the values become smaller.

Finally, the value of the gap g is estimated as the distance between the upper side of the box and the top side G of the second sphere.

4. Variational model

The variational model in [17] has been considered and implemented in this work.

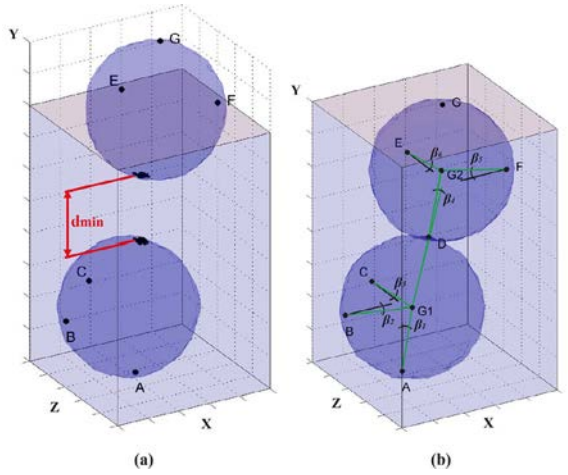

Fig. 4. a) Minimum distance between the two spherical clouds, b) β_i angles to evaluate if each spherical cloud is stable (amplified 100 times)

The assembly graph of Fig. 5 shows three joints of spherical slider kind between the box and the first sphere SPH_1 at points A, B and C, one joint of spherical kind between the sphere SPH_1 and the sphere SPH_2 at point D, two joints of spherical slider kind between the sphere SPH_2 and the box at point F and E [13] and the measure to perform *g*.

A Datum Reference Frame (DRF) has been assigned to each feature of each part and to the whole assembly (see Fig. 1). The DRF X-Y-Z of the box in Fig. 3 is also considered as the global DRF of the assembly.

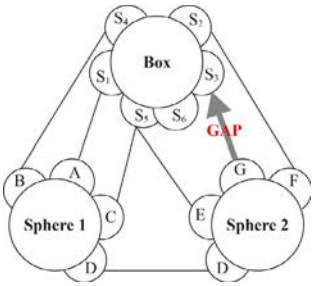

Fig. 5. Assembly graph of case study

Once located the DRF's, the model parameters can be assigned and it is possible to evaluate the equations of the features in the global DRF of the assembly:

$$S_1: -r_{z01}X + Y + r_{x01}Z + \left(25r_{z01} - 25r_{x01} - t_{y01}\right) = 0 \quad (5)$$

$$S_2: -X - r_{z02}Y + r_{x02}Z + \left(40r_{z02} - 25r_{x02} + \left(50 - t_{y02}\right)\right) = 0 \quad (6)$$

$$S_3: r_{z03}X - Y + r_{x03}Z + \left(-25r_{z03} - 25r_{x03} + \left(80 - t_{y01}\right)\right) = 0 \quad (7)$$

$$S_4: X + r_{z04}Y + r_{x04}Z + \left(-25r_{x04} - 40r_{xz04} - t_{y04}\right) = 0 \quad (8)$$

$$S_5: -r_{z05}X - r_{x05}Y + Z + \left(40r_{x05} + 25r_{xz05} - t_{y05}\right) = 0 \quad (9)$$

$$S_6: -r_{z06}X + r_{x06}Y - Z + \left(25r_{xz06} - 40r_{x06} + 50 - t_{y06}\right) = 0 \quad (10)$$

$$SPH_1: \quad \left(X_1 - \Delta X_{12} - O_{12X}\right)^2 + \left(Y_1 - \Delta Y_{12} - O_{12Y}\right)^2 = \left(R_1 + r_1 + d_1\right)^2 \quad (11)$$

$$SPH_2: \quad \left(X_1 - \Delta X_{13} - O_{13X}\right)^2 + \left(Y_1 - \Delta Y_{13} - O_{13Y}\right)^2 = \left(R_2 + r_2 + d_2\right)^2 \quad (12)$$

where r_{zi} are the rotation parameters of the generic features S_i measured in their Datum Reference Frame (DRF in Fig. 1), t_{yi} are the translation parameters of the generic features S_i in their DRF, r_1 is the model parameter, due to the dimensional tolerances, of the first sphere SPH_1, r_2 is the model parameter, due to the dimensional tolerances, of the second sphere SPH_2, d_1 and d_2 are the model parameters due to the form tolerance applied to the first and the second sphere respectively, ΔX_{12}, ΔY_{12} and ΔZ_{12} are the assembly parameters of the first sphere, ΔX_{13}, ΔY_{13} and ΔZ_{13} are the assembly parameters of the second sphere in the box. The parameters r_{zi} and t_{yi} of the features of the box are equal to zero, since the box has been considered nominal.

Once all the features are expressed in the same global DRF of the assembly, the assembly is created by imposing the assembly conditions. As showed by the assembly graph, the functional requirement *g* must be measured between the feature S_3 of the box and the G point of the second sphere SPH_2. The equation of S_3 in the global DRF of the assembly is known by eq. (7), the equation of SPH_2 in the global DRF of the assembly is unknown since eq. (12) have the assembly parameters that are unknown. To calculate the assembly parameters it is needed to investigate firstly the assembly between the box and the first sphere and, then, the assembly among the second sphere and the sub-assembly between the box and the first cloud.

The first sphere SPH_1 is assembled with the features S_1, S_4 and S_5 of the box by means of three spherical slider constrain equations:

$$SPH_1\text{-}S_1: \quad \begin{aligned} &-r_{z01}\left(\Delta X_{12} + 20\right) + \left(\Delta Y_{12} + 20\right) + r_{x01}\left(\Delta Z_{12} + 20\right) + \\ &+\left(25r_{z01} - 25r_{x01} - t_{y01}\right) - \left(20 + r_1 + d_1\right) = 0 \end{aligned} \quad (13)$$

$$SPH_1\text{-}S_4: \quad \begin{aligned} &\left(\Delta X_{12} + 20\right) + r_{z04}\left(\Delta Y_{12} + 20\right) + r_{x04}\left(\Delta Z_{12} + 20\right) + \\ &+\left(-25r_{x04} - 40r_{z04} - t_{y04}\right) - \left(20 + r_1 + d_1\right) = 0 \end{aligned} \quad (14)$$

$$SPH_1\text{-}S_5: \quad \begin{aligned} &-r_{z05}\left(\Delta X_{12} + 20\right) - r_{z05}\left(\Delta Y_{12} + 20\right) + \left(\Delta Z_{12} + 20\right) + \\ &+\left(40r_{x05} + 25r_{z05} - t_{y05}\right) - \left(20 + r_1 + d_1\right) = 0 \end{aligned} \quad (15)$$

The solution of eqs. (13)-(15) allows to calculate the assembly parameters of the first sphere on the box:

$$\Delta X_{12} = R_1 + d_B + r_1 - 20 \tag{16}$$

$$\Delta Y_{12} = R_1 + d_A + r_1 - 20 \tag{17}$$

$$\Delta Z_{12} = R_1 + d_c + r_1 - 20 \tag{18}$$

where d_i are the model parameters due to the form tolerance applied to the spheres (where i=A, B, C, D, E, F and G with A, B, C, E and F are the contact points between the spheres and the box as shown in Fig. 3).

The second sphere SPH_2 is assembled with the sub-assembly constituted by the box and SPH_1 through two spherical slider constrain joints, between SPH_2 and S_2 and between SPH_2 and S_5, and a spherical-spherical constrain joint between SPH_2 and SPH_1. The three constrain equations are:

$$\begin{aligned} &\text{SPH}_2\text{-S}_2\text{:} \\ &-(\Delta X_{13}+30)-r_{z02}(\Delta Y_{13}+58{,}73)+r_{x02}(\Delta Z_{13}+20)+ \\ &+(50+40r_{z02}-R_2-r_2-d_2-25r_{x02}-t_{y02})=0 \end{aligned} \tag{19}$$

$$\begin{aligned} &\text{SPH}_2\text{-S}_5\text{:} \\ &-r_{z05}(\Delta X_{13}+30)-r_{x05}(\Delta Y_{13}+58{,}73)+(\Delta Z_{13}+20)+ \\ &+(50+40r_{x05}-R_2-r_2-d_2+25r_{z05}-t_{y05})=0 \end{aligned} \tag{20}$$

$$\begin{aligned} &\text{SPH}_2\text{-S}_1\text{:} \\ &(\Delta X_{13}-\Delta X_{12}+10)^2+(\Delta Y_{13}-\Delta Y_{12}+38{,}73)^2+ \\ &(\Delta Z_{13}-\Delta Z_{12})^2-(R_1+R_2+r_1+r_2+d_1+d_2)^2=0 \end{aligned} \tag{21}$$

The solution of eqs. (19)-(21) allow to calculate the assembly parameters of the second sphere on the sub-assembly constituted by the box and SPH_1:

$$\Delta X_{13} = 20 - d_F - r_2 - R_2 \tag{22}$$

$$\begin{aligned} \Delta Y_{13} &= R_1 + d_A + r_1 + (100R_1 + 20R_2 + 60d_B + 40d_c - 40d_E + \\ &+ 60d_F + 100r_1 + 20r_2 + 2R_1R_2 - 2R_1d_B - 2R_1d_C + 2R_1d_{D1} + \\ &+ 2R_1d_{D2} + 2R_2d_{D1} + 2R_2d_{D2} - 2R_1r_1 + 2R_1r_2 + 2R_2r_1 + \\ &+ 2R_2r_2 + 2d_{D1}d_{D2} - 2d_Br_1 - 2d_Cr_1 + 2d_{D1}r_1 + 2d_{D2}r_1 + \\ &+ 2d_{D1}r_2 + 2d_{D2}r_2 + 2R_1\Delta z_{12} - 2R_1(-\Delta X_{12}) + 2r_1r_2 + \\ &- d_B(-2\Delta X_{12}) + d_C(2\Delta Z_{12}) + r_1(2\Delta Z_{12}) - r_1(-2\Delta X_{12}) + \\ &- R_1^2 + R_2^2 - d_B^2 - d_C^2 + d_{D1}^2 + d_{D2}^2 - r_1^2 + r_2^2 - (\Delta Z_{12})^2 + \\ &- (\Delta X_{12})^2 - 1700)^{0.5} - 5{,}873 \end{aligned} \tag{23}$$

$$\Delta Z_{13} = R_2 + d_E + r_2 - 20 \tag{24}$$

The functional requirement g between SPH_2 and S_3 may be evaluated by means of the analytical equation to evaluate the minimum oriented distance between a plane and a sphere, that is:

$$g = n_x c_x + n_y c_y + n_z c_z - (R_2 + r_2 + d_G) \tag{25}$$

where n_x, n_y, n_z are the coefficients of the equation of the plane and c_x, c_y and c_z are the coordinates of the center of the sphere. By substituting the model parameters of the plane and the sphere in eq. (19), it is possible to obtain the following equation:

$$g = 1{,}27 + 20 - \Delta Y_{13} - R_2 - r_2 - d_G \tag{26}$$

4.1 Manufacturing signature and operating conditions

The variational model with manufacturing signature and operating conditions starts by generating spheres by means of eq. (1). Those spheres are randomly rotated and they are assembled to the box, as previously done for the geometrical approach. Once verified that the positions of the two spheres are stable, by taking into account the weight and the friction forces applied to the spheres, the coordinates of the contact points are identified. The coordinates of the contact points are transformed into coordinates associated to the DRF of each sphere. Then, they are used to enter inside the array of the generated point-cloud to read the corresponding form deviations. The values of the model parameter of the points of contact have been substituted into eqs. (23) and (26).

5. Results comparison and discussion

Monte Carlo simulation has been carried out by implementing 10.000 runs.

The boxplots in Fig. 6 show results of the measured gap g for all the models (model 1 is the geometrical approach, model 2 is the variational model, model 3 is the variational model with manufacturing signature and operating conditions). The same figure reports the nominal value of the gap g (equal to 1,2702 mm), the boxplots of the gap g as result by the Monte Carlo simulations and the tolerance range due to the worst case approach (classical approach in tolerance analysis). All the three models give a distribution of the gap g completely contained inside the worst case tolerance range.

The normality of the obtained distributions of the gap g has been evaluated by means of Anderson-Darling test. The results are reported in Table 1 together with mean, standard deviation, Skewness, Kurtosis and simulation time.

Model 1 (i.e. geometrical model) is considered the reference case.

Model 3 (i.e. variational model with manufacturing signature and operating conditions) is very near to model 1 in terms of both mean value and standard deviation.

Model 2 (i.e. pure variational model) overestimates slightly the mean value of the g gap, even if it is negligible. It underestimates the standard deviation of about:

$$\frac{\sigma_2 - \sigma_1}{\sigma_1} * 100 = 17{,}6\% \tag{27}$$

This is due to the fact that model 2 does not take into account the correlation among the points of the spheres.

Levene test testifies that the difference between the standard deviations of models 2 and 1 respectively is statistically significative, as shown in Fig. 7.

Model 1 and 3 have comparable simulation times (108.000 s) that are significantly higher than the time required for simulation 2 (few seconds). Therefore, model 2 appears a good choice in terms of simulation time, if it is possible to neglect a decrease of about 17,6% in the estimation of gap *g*.

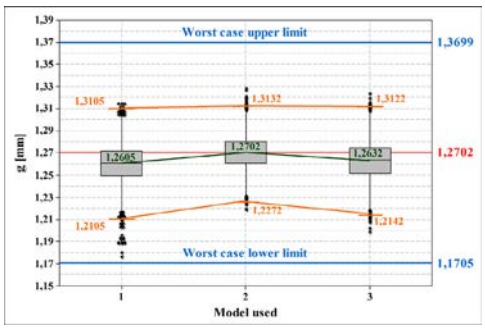

Fig. 6. Results of the measured gap *g*

Table 1. Simulation results (10.000 runs)

Model	Mean [mm]	σ [mm]	A-Squared	P-value	Skew.	Kurt.
1	1,2605	0,017	1,94	0,005	-0,241	1,666
2	1,2702	0,014	0,43	0,309	0,017	-0,001
3	1,2632	0,016	0,62	0,108	-0,005	-0,127

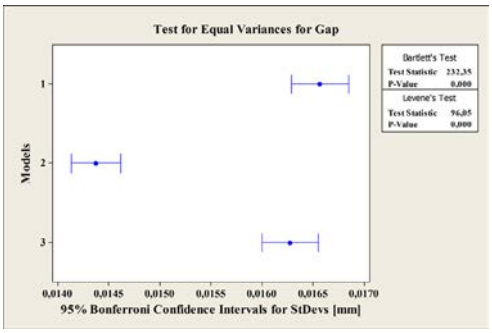

Fig. 7. Results of Levene's test

6. Conclusions

The effort of this work has been to include in the approaches for tolerance analysis the manufacturing signature and the operating conditions during assembly.

The results show that a model of the literature, the variational one, with manufacturing signature and operating conditions allows to better reproduce the actual assembling of machined spheres in presence of weight and friction forces. In fact, the mean value and the standard deviation of this model are statistically equal to those of the geometrical approach that considers manufacturing signature and operating conditions. The variational model without the manufacturing signature and the operating conditions underestimates the tolerance range of the gap g of about 17,6%, even if its simulation time is of only few seconds.

The drawback of all the models that involves manufacturing signature and operating conditions is the simulation times. It is currently matter of further study.

References

[1] Chen H, Jin S, Li Z, Lai X. A comprehensive study of three dimensional tolerance analysis methods. Comp Aid Des 2014; 53:1-13.
[2] Polini W, Geometric Tolerance Analysis. In: Colosimo BM, Senin N, editors. Impact on Product Design, Quality Inspection and Statistical Process Monitoring. London:Springer; 2011. p.39-68.
[3] Bo C, Yng Z, Wang L, Chen H. A comparison of tolerance analysis models for assembly. Int J Adv Manuf Technol 2013; 68:739-754.
[4] Ameta G, Serge S, Giordano M. Comparison of spatial math models for tolerance analysis: tolerance maps, deviation domain, and TTRS. J Comput Inf Sci Eng 2011; 11:021004.
[5] Polini W. Taxonomy of models for tolerance analysis in assembling. Int J Prod Res 2012; 50:2014-2029.
[6] Samper S, Adragna PA, Favreliere H, Pillet M. Modeling of 2D and 3D assemblies taking into account form errors of plane surfaces. Journal of Computing and Information Science in Engineering 2009; 9:041005.
[7] Stoll T, Wittmann S, Helwig S, Petzold K. Registration of meaured and simulated non-ideal geometry using optimization methods. In: Weckenmann A, editor. Proceedings of the 10th CIRP International Seminar on Computer Aided Tolerancing. Erlagen; 2007. Paper No. BV1.
[8] Stoll T, Wittmann S, Meerkamm H. Tolerance analysis with detailed part modeling including shape deviations. In: Giorndano M, Villeneuve F, Mathieu L, editors. Proceedings of the 11th CIRP International Conference on Computer Aided Tolerancing, Annecy; 2009. Paper No. C5-1.
[9] Schleich B, Anwer N, Mathieu L, Wartzack S. Skin Model Shapes: A new paradigm shift for geometric variations modeling in mechanical engineering. Computer-Aided Design 2014;50:1–15.
[10] Anwer N, Schleich B, Mathieu L, Wartzack S. From solid modeling to skin model shapes: Shifting paradigms in computer-aided tolerancing. CIRP Annals – Manufacturing Technology 2014;63(1):137–140.
[11] Weihua N, Zhenqiang Y. Integrating cylindricity error into tolerance analysis of precision rotary assemblies using Jacobian-Torsor model. Proc. IMechE Part C: J Mech Eng Scie 2013; 227(11): 2517-2530.
[12] Moroni G, Polini W. Tolerance based variation in solid modelling. J Comp Inf Sc in Eng, 2003; 3(4): 345-352.
[13] Martino PM, Gabriele GA. Application of Variational Geometry to the Analysis of Mechanical Toleranced. Conference on Failure Prevention and Reliability ASME Paper 1989; 16:19–27.
[14] Boyer M, Stewart NF. Modeling Spaces for Toleranced Objects. Int J Robot Res 1991;10(5):570-582.
[15] Gupta S, Turner JU. Variational Solid Modelling for Tolerance Analysis. IEEE Comput Graphics Appl 1993;13:64–74.
[16] Corrado A, Polini W, Moroni G. Manufacturing signature and operating conditions for tolerance analysis. Proceedings XII AITeM Conference, Palermo, Italy, September 7-9, 2015.
[17] Marziale M, Polini W, A new model based on variational solid modelling. Proceedings of the ASME 2010 10th Biennial Conference on Engineering Systems Design and Analysis, ESDA 2010, Instanbul, Turkey , July 12-14, 2010.